BEDT–TTF SALTS WITH SQUARE PLATINATES(II) AS COUNTERIONS: [BEDT–TTF]$_4$[Pt(C$_2$O$_4$)$_2$], A NEW ORGANIC METAL

S. GÄRTNER, I. HEINEN and D. SCHWEITZER

Max-Planck-Institut für Medizinische Forschung, AG Molekülkristalle, Jahn-Strasse 29, 6900 Heidelberg (F.R.G.)

B. NUBER and H. J. KELLER

Anorganisch-Chemisches Institut der Universität Heidelberg, Im Neuenheimer Feld 270, 6900 Heidelberg (F.R.G.)

Abstract

The title compound, [BEDT–TTF]$_4$[Pt(C$_2$O$_4$)$_2$], is obtained by electrocrystallization, which yields black platelets of stoichiometry C$_{44}$H$_{32}$O$_8$PtS$_{32}$, M_r = 1909.87. Crystal structure determination at room temperature gives a triclinic cell P$\bar{1}$, with a = 8.678(2) Å, b = 11.878(5) Å, c = 15.757(7) Å, α = 105.49(3)°, β = 91.05(3)°, γ = 91.96(3)°, V = 1563.64 Å^3, d_c = 2.03 g/cm^3, Z = 1. The solid contains sheets of BEDT–TTF cations separated by sheets of [Pt(C$_2$O$_4$)$_2$]$^{2-}$ counterions. The BEDT–TTF sheets are made up of columns that interact strongly through S–S contacts. The columns are built up by pairs of BEDT–TTF molecules. There are strongly varying bond distances in the two different BEDT–TTF moieties that make up a pair. This fact is especially clearly expressed in the surprisingly short C—C distances of the central C=C double bond of the two BEDT–TTF ions: 1.273 Å and 1.327 Å respectively. These are by far the shortest distances for the central C=C bonds observed so far in conductive BEDT–TTF salts. The compound behaves like a metal down to about 60 K. Temperature-dependent d.c. conductivity, e.s.r. and thermopower measurements show *metallic* behaviour at room temperature (σ_{300} = 20 S/cm) with a metal-to-metal phase transition around 200 K. At about 60 K a second *broad* phase transition occurs and the crystals become semiconducting.

Introduction

The combination of BEDT–TTF$^+$ radical cations with anions of transition metal complexes has proven to be exceptionally successful in the search for new molecular metals [1 - 7] and superconductors [1, 7 - 9]. The organic conductor with the highest transition temperature to superconductivity so far observed, 10.4 K in [BEDT–TTF]$_2$[Cu(SCN)$_2$] [8, 9], belongs to this group of solids.

For several reasons we have decided to combine two successful principles in one solid: the properties of the 'inorganic', one-dimensional, *molecular metals*, which were of central interest a decade ago because of their potential to form *one-dimensionally* interacting transition metal ion chains (typically in mixed valence platinates [10 - 12]) on one hand and the special often pronounced *two-dimensional* properties of metallic, organic solids containing radical cations like BEDT–TTF$^+$ on the other hand. Recently we obtained two phases of [BEDT–TTF]$_4$[Pt(CN)$_4$] as the first solids in our efforts to combine lattice elements of typical 'inorganic' with those of well-known 'organic' *molecular metals* [13]. One of them turned out to be semi-conducting at room temperature and below while the second is metallic at room temperature [13]. In this communication we report the preparation, structure and some physical properties of a *metallic* phase of another compound from this class of materials, namely [BEDT–TTF]$_4$[Pt(C$_2$O$_4$)$_2$].

Experimental

Preparation

The crystals of 1 were obtained by electrocrystallization. In a typical experiment 60 mg of BEDT–TTF were dissolved in 100 ml warm 1,1,2-trichloroethane. To this solution was added 225 mg of K$_2$[Pt(C$_2$O$_4$)$_2$] finely ground in a mortar and the mixture was stirred for several hours. Finally, 1000 mg of 18-crown-6-ether were added. The mixture was put into a three-compartment cell without filtering and electrolysed for about five weeks using a voltage of 1.8 V, resulting in a current of 0.3 to 0.5 μA. This dark crystals of the title compound are obtained.

X-ray structure

A dark brownish black prismatic crystal, $0.05 \times 0.2 \times 0.2$ mm^3, was used for the structure determination. Lattice parameters were obtained from setting angles of 25 reflections ($3 < 2\theta < 35°$) centred on a diffracto-meter (Syntex R3, Mo Kα radiation). Data collection at room temperature by Ω scan ($3 < 2\theta < 60°$) yielded 4577 observed independent reflections with $I > 2.5 \sigma (I)$. An empirical absorption correction using psi-scans of five reflections with $6 < 2\theta < 27°$ was applied ($\mu = 33.5$ cm^{-1}). The structure was solved by direct methods and Fourier syntheses. Refinement of 385 variables (fixed hydrogen positions) converged with $R = 0.055$ and $R_w = 0.047$. The largest features in a final Fourier map were $+0.94$ and -1.96 eA^{-3}.

Calculations were performed with the SHELXTL program package [14] on an Eclipse computer (Data General) using scattering factors from the *International Tables of X-ray Crystallography* [15].

Physical measurements

Temperature-dependent resitivity measurements were carried out with the typical four-probe technique in the temperature range 4.2 - 300 K.

Thermopower measurements were done with an apparatus described earlier [16] in the same temperature range. The e.s.r. investigations were performed with an X-band spectrometer (Bruker ESP 300) from 4.2 to 300 K. A single e.s.r. line was observed, as is typical for conduction electrons of a metal. The spin susceptibility was obtained in the usual way from the e.s.r. linewidth and the intensity of the signal. The unit cell data of the crystals used for the measurements of the physical properties were controlled by X-ray (after the measurements).

Results

Atomic coordinates are listed in Table 1, bond distances and angles in Table 2. Figure 1 shows the two crystallographically different BEDT–TTF moieties of the unit cell and Fig. 2 the $[Pt(C_2O_4)_2]^{2-}$ counterion. The numbering scheme is indicated in these Figures. The two different BEDT–TTF molecules occur in pairs, which make up columns. Projections of the unit cell along (Fig. 3) and perpendicular (Fig. 4) to these columns give an impression of the 'pairing' and they show that there are strong S—S contacts
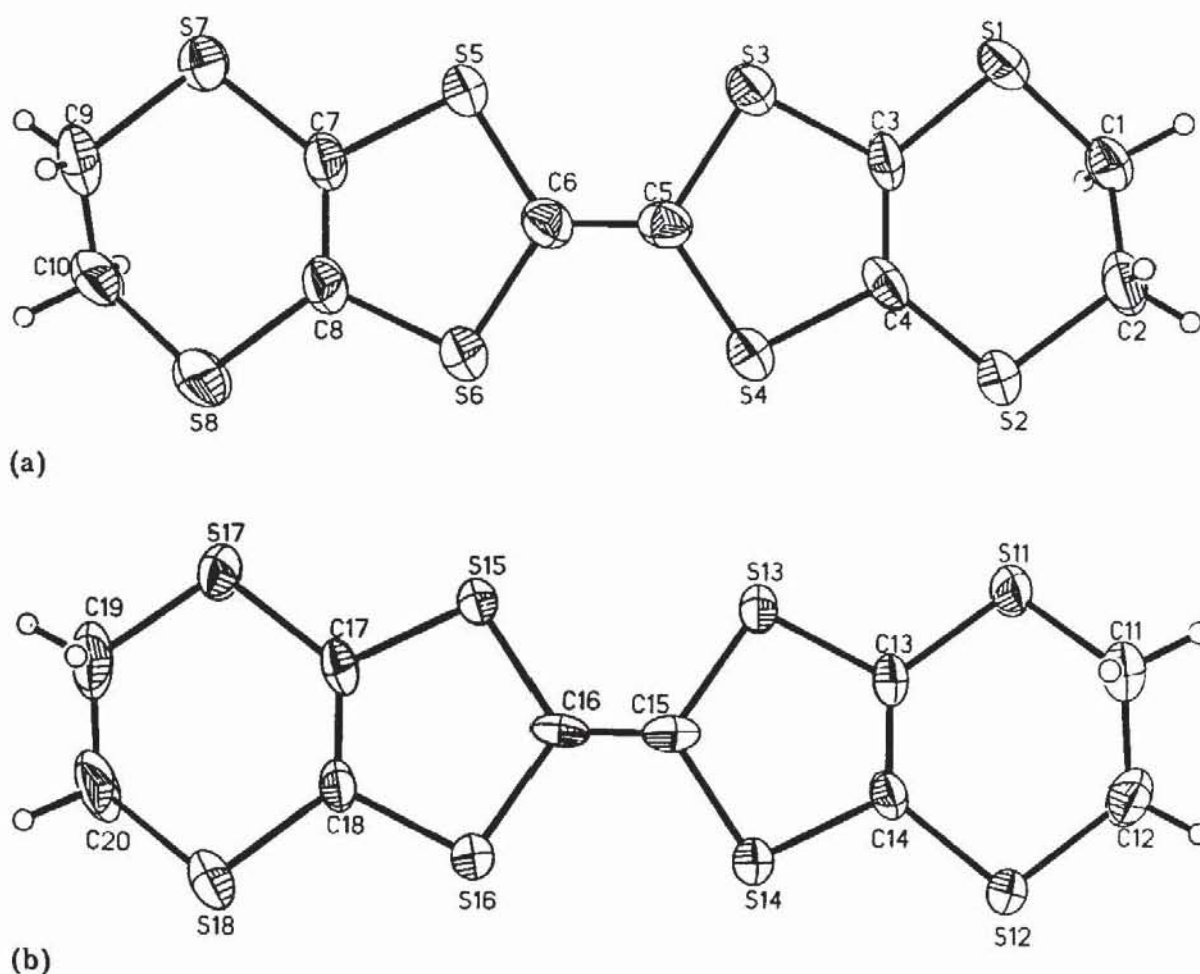

Fig. 1. Numbering schemes (a) and (b) of the two crystallographically different BEDT–TTF moieties.

TABLE 1

Atomic coordinates

Atom	x/a	y/b	z/c	Atom	x/a	y/b	z/c
PT1	.00000	.50000	.50000	H2A	.47302	.52139	1.42490
	.00000	.00000	.00000		.00099	.00074	.00055
O1	.20511	.42076	.47165	H2B	.57220	.44107	1.34330
	.00058	.00044	.00035		.00099	.00074	.00055
O2	.07034	.34444	.50128	C3	.32771	.28299	1.21187
	.00061	.00045	.00037		.00094	.00070	.00050
O3	-.31305	.25430	.50683	C4	.31834	.37729	1.21272
	.00068	.00047	.00037		.00091	.00068	.00049
O4	.02025	.16443	.49771	C5	.19792	.28018	1.06061
	.00069	.00050	.00045		.00094	.00064	.00051
C21	.20710	.31320	.47995	C6	.11900	.24678	.78458
	.00101	.00070	.00050		.00093	.00066	.00053
C22	.03922	.26447	.49867	C7	-.01509	.13011	.83963
	.00099	.00072	.00055		.00098	.00071	.00051
O1	.37519	.22564	1.27363	C8	-.02138	.24484	.83870
	.00034	.00020	.00016		.00098	.00071	.00053
O2	.36196	.52049	1.29043	C9	-.14912	.06334	.67393
	.00031	.00020	.00016		.00134	.00083	.00058
O3	.26615	.17895	1.11550	H9A	.22606	.00866	.64033
	.00031	.00019	.00015		.00134	.00083	.00058
O4	.24581	.42437	1.11645	H9B	-.06258	.06781	.63771
	.00029	.00019	.00014		.00134	.00083	.00058
O5	.07189	.10197	.93141	C10	-.21075	.17898	.69615
	.00032	.00019	.00015		.00118	.00075	.00063
O6	.05533	.34697	.93127	H10A	-.24207	.19637	.64241
	.00030	.00020	.00015		.00117	.00074	.00063
O7	-.08336	.00662	.75945	H10B	-.30029	.17276	.72972
	.00037	.00021	.00018		.00117	.00074	.00063
O8	.10245	.29730	.75803	O11	.30718	.26715	.65784
	.00036	.00022	.00019		.00033	.00019	.00015
C1	.40470	.35221	1.38739	O12	.34703	-.02460	.64960
	.00108	.00068	.00052		.00036	.00019	.00016
H1A	.46304	.33407	1.43605	O13	.44612	.31306	.83812
	.00108	.00068	.00052		.00027	.00018	.00014
H1B	.30136	.36941	1.40795	O14	.46706	.06562	.83114
	.00108	.00068	.00052		.00029	.00018	.00014
C2	.47538	.46193	1.37049	O15	.63224	.38211	1.02672
	.00099	.00074	.00055		.00028	.00018	.00014

(continued)

TABLE 1 (*continued*)

Atomic coordinates

| Atom	x/a	y/b	z/c	Atom	x/a	y/b	z/c
S16	.65162	.13367	1.01660	C15	.51211	.21045	.87223
	.00029	.00018	.00015		.00091	.00060	.00054
S17	.79564	.46560	1.19777	C16	.58620	.23774	.96584
	.00032	.00017	.00015		.00090	.00061	.00056
S18	.02542	.16739	1.18240	C17	.72661	.34674	1.11337
	.00035	.00022	.00017		.00089	.00070	.00047
C11	.34637	.15343	.56356	C18	.73572	.23197	1.10812
	.00102	.00068	.00052		.00094	.00070	.00050
H11A	.43614	.14634	.56058	C19	.71194	.37818	1.26353
	.00102	.00068	.00051		.00114	.00090	.00061
H11B	.30819	.17311	.51199	H19A	.72616	.45252	1.32063
	.00102	.00068	.00051		.00114	.00090	.00060
C12	.27833	.03680	.56591	H19B	1.00782	.38475	1.23594
	.00108	.00070	.00055		.00114	.00090	.00060
H12A	.16974	.04681	.57380	C20	.85689	.28554	1.27525
	.00108	.00070	.00055		.00138	.00082	.00057
H12B	.29458	-.01819	.51020	H20A	.72902	.26214	1.31359
	.00108	.00070	.00055		.00138	.00082	.00057
C13	.37698	.21135	.74185	H20B	.75766	.27764	1.30350
	.00091	.00068	.00049		.00138	.00082	.00057
C14	.38955	.09822	.73830				
	.00094	.00069	.00050				
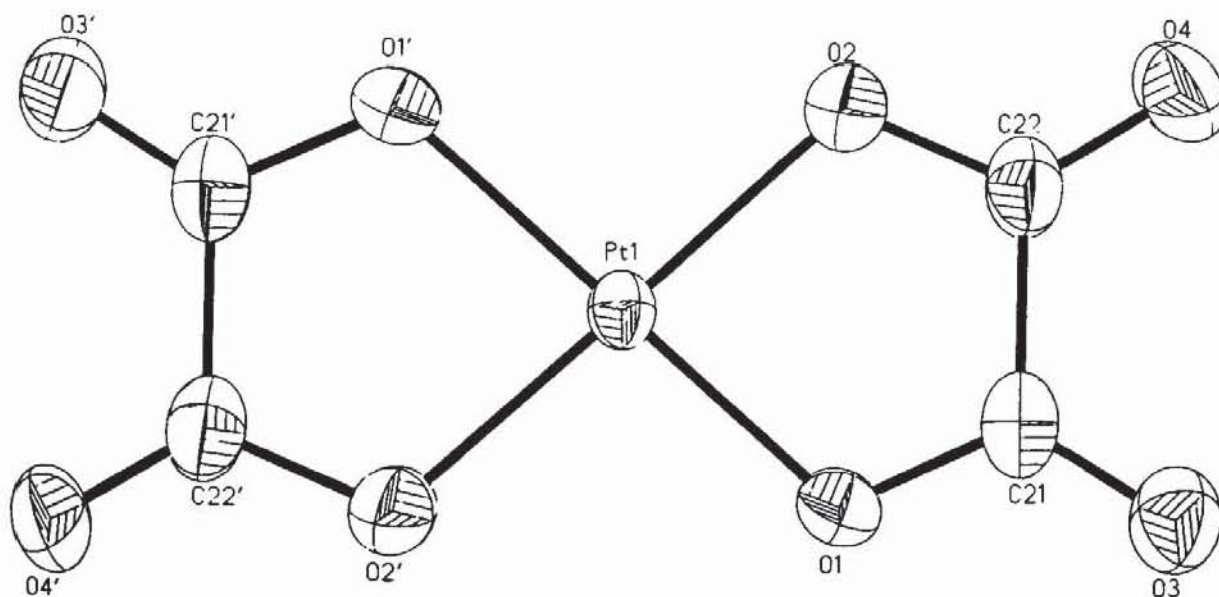
Fig. 2. Numbering scheme of the $[Pt(C_2O_4)_2]^{2-}$ counterions.

TABLE 2

Bond lengths (Å) and bond angles (°)

```
PT1 -O1    1.970( .005)
PT1 -O2    1.971( .006)   82.6( .2)
PT1 -O1 A  1.970( .005)  180.0( .0)    97.4( .2)
PT1 -O2 A  1.971( .006)   97.4( .2)   180.0( .0)   82.6( .2)
                            O1            O2           O1 A
O1  -PT1   1.970( .005)
O1  -C21   1.320( .010)  113.9( .5)
                            PT1
O2  -PT1   1.971( .006)
O2  -C22   1.313( .010)  115.6( .5)
                            PT1
O3  -C21   1.200( .011)

O4  -C22   1.202( .011)

C21 -O1    1.320( .010)
C21 -O3    1.200( .011)  124.8( .8)
C21 -C22   1.544( .012)  114.5( .7)   120.6( .8)
                            O1            O3
C22 -O2    1.313( .010)
C22 -O4    1.202( .011)  125.8( .8)
C22 -C21   1.544( .012)  112.5( .7)   121.6( .8)
                            O2            O4
S1  -C1    1.803( .007)
S1  -C3    1.739( .009)  102.3( .4)
                            C1
S2  -C2    1.780( .010)
S2  -C4    1.729( .007)  101.6( .4)
                            C2
S3  -C3    1.744( .007)
S3  -C5    1.769( .009)   95.9( .4)
                            C3
S4  -C4    1.747( .009)
S4  -C5    1.736( .007)   97.1( .4)
                            C4
S5  -C6    1.733( .007)
S5  -C7    1.734( .009)   95.6( .4)
                            C6
S6  -C6    1.727( .009)
S6  -C8    1.732( .008)   96.1( .4)
                            C6
S7  -C7    1.738( .008)
S7  -C9    1.755( .011)  103.4( .4)
                            C7
S8  -C8    1.725( .010)
S8  -C10   1.735( .009)  101.8( .5)
                            C8
C1  -S1    1.803( .007)
C1  -H1A    .960( .000)  108.7( .3)
C1  -H1B    .960( .000)  108.1( .3)   109.5( .0)
C1  -C2    1.524( .013)  114.1( .6)   109.4( .5)   107.0( .5)
                            S1            H1A          H1B
H1A -C1     .960( .000)

H1B -C1     .960( .000)

C2  -S2    1.780( .010)
C2  -C1    1.524( .013)  114.6( .6)
C2  -H2A    .960( .000)  108.4( .3)   109.4( .4)
```

(continued)

TABLE 2 (*continued*)

Bond lengths (Å) and bond angles (°)

```
C2  -H2B   .960( .000)   108.0( .3)   107.0( .5)   109.5( .0)
                            S2           C1           H2A
H2A -C2    .960( .000)

H2B -C2    .960( .000)

C3  -S1   1.739( .009)
C3  -S3   1.744( .007)   114.8( .5)
C3  -C4   1.359( .012)   128.0( .6)   117.2( .6)
                            S1           S3
C4  -S2   1.729( .007)
C4  -S4   1.746( .009)   115.2( .5)
C4  -C3   1.359( .012)   128.8( .6)   116.0( .5)
                            S2           S4
C5  -S3   1.769( .009)
C5  -S4   1.736( .007)   113.0( .4)
C5  -C6   1.326( .011)   122.4( .6)   124.6( .7)
                            S3           S4
C6  -S5   1.733( .007)
C6  -S6   1.727( .009)   115.1( .5)
C6  -C5   1.326( .011)   123.2( .7)   121.8( .6)
                            S5           S6
C7  -S5   1.734( .009)
C7  -S7   1.738( .008)   114.8( .5)
C7  -C8   1.369( .012)   116.9( .6)   128.3( .7)
                            S5           S7
C8  -S6   1.732( .008)
C8  -S8   1.725( .010)   116.4( .5)
C8  -C7   1.369( .012)   116.2( .7)   127.4( .6)
                            S6           S8
C9  -S7   1.755( .011)
C9  -H9A   .960( .000)   107.2( .3)
C9  -H9B   .960( .000)   107.1( .4)   109.5( .0)
C9  -C10  1.448( .013)   118.7( .7)   108.7( .6)   105.4( .6)
                            S7           H9A          H9B
H9A -C9    .960( .000)

H9B -C9    .960( .000)

C10 -S8   1.735( .009)
C10 -C9   1.448( .013)   121.0( .8)
C10 -H10A  .960( .000)   107.1( .4)   108.2( .5)
C10 -H10B  .960( .000)   105.9( .3)   104.9( .6)   109.5( .0)
                            S8           C9           H10A
H10A-C10   .960( .000)

H10B-C10   .960( .000)

S11 -C11  1.781( .007)
S11 -C13  1.753( .009)   100.3( .4)
                            C11
S12 -C12  1.772( .010)
S12 -C14  1.753( .007)   103.3( .4)
                            C12
S13 -C13  1.749( .007)
S13 -C15  1.768( .009)    96.7( .4)
                            C13
S14 -C14  1.740( .009)
```

TABLE 2 (*continued*)

Bond lengths (Å) and bond angles (°)

```
S14 -C15   1.759( .007)   97.1( .4)
                          C14
S15 -C16   1.755( .007)
S15 -C17   1.731( .009)   96.3( .4)
                          C16
S16 -C16   1.746( .009)
S16 -C18   1.726( .007)   96.3( .4)
                          C16
S17 -C17   1.741( .007)
S17 -C19   1.785( .011)  102.7( .4)
                          C17
S18 -C18   1.747( .009)
S18 -C20   1.746( .008)  102.4( .4)
                          C18
C11 -S11   1.781( .007)
C11 -H11A   .960( .000)  108.1( .3)
C11 -H11B   .960( .000)  108.6( .3)   109.5( .0)
C11 -C12   1.497( .012)  114.0( .6)   107.1( .5)   109.5( .5)
                          S11         H11A         H11B

H11A-C11    .960( .000)

H11B-C11    .960( .000)

C12 -S12   1.772( .010)
C12 -C11   1.497( .012)  117.6( .6)
C12 -H12A   .960( .000)  107.3( .3)   106.2( .5)
C12 -H12B   .960( .000)  107.6( .3)   108.4( .4)   109.5( .0)
                          S12         C11          H12A

H12A-C12    .960( .000)

H12B-C12    .960( .000)

C13 -S11   1.753( .009)
C13 -S13   1.749( .007)  116.1( .5)
C13 -C14   1.333( .012)  126.9( .6)   116.9( .6)
                          S11         S13
C14 -S12   1.753( .007)
C14 -S14   1.740( .009)  114.1( .5)
C14 -C13   1.338( .012)  128.7( .7)   117.1( .6)
                          S12         S14
C15 -S13   1.768( .009)
C15 -S14   1.759( .007)  112.0( .4)
C15 -C16   1.273( .011)  124.2( .6)   123.8( .7)
                          S13         S14
C16 -S15   1.755( .007)
C16 -S16   1.746( .009)  113.2( .5)
C16 -C15   1.273( .011)  124.0( .7)   122.8( .6)
                          S15         S16
C17 -S15   1.731( .009)
C17 -S17   1.741( .007)  115.4( .5)
C17 -C18   1.351( .012)  116.7( .5)   128.0( .6)
                          S15         S17
C18 -S16   1.726( .007)
C18 -S18   1.747( .009)  114.3( .5)
C18 -C17   1.351( .012)  117.4( .6)   128.2( .6)
                          S16         S18
C19 -S17   1.785( .011)
C19 -H19A   .960( .000)  107.4( .3)
C19 -H19B   .960( .000)  107.2( .3)   109.5( .0)
```

TABLE 2 (*continued*)

Bond lengths (Å) and bond angles (°)

C19 –C20	1.464(.015)	118.0(.7)	108.4(.5)	106.1(.6)	
		S17	H19A	H19B	
H19A–C19	.960(.000)				
H19B–C19	.960(.000)				
C20 –S18	1.746(.008)				
C20 –C19	1.464(.015)	118.9(.7)			
C20 –H20A	.960(.000)	107.3(.4)	108.3(.6)		
C20 –H20B	.960(.000)	106.8(.4)	105.8(.6)	109.5(.0)	
		S18	C19	H20A	
H20A–C20	.960(.000)				
H20B–C20	.960(.000)				
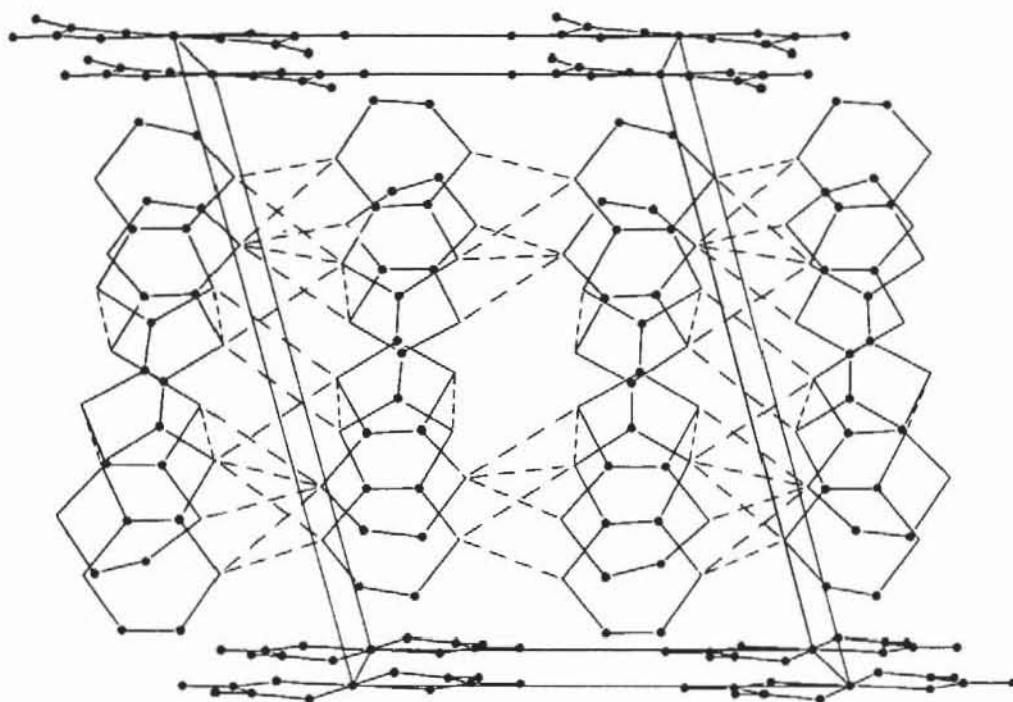
Fig. 3. Section of the structure projected along the columns. Dotted lines represent intermolecular S....S contacts < 3.8 Å.

between molecules of the different columns. Figure 5 gives a different view of the intermolecular S–S contacts between BEDT–TTF moieties of different columns. The dotted lines in Figs. 3, 4 and 5 connect S atoms that are less than 3.8 Å apart. 3.6 Å is the sum of the covalent S radii [17].

The bond distances in the two different BEDT–TTF molecules of a pair vary appreciably. Especially pronounced is this difference in the bond distances of the central C=C bond. It is 1.273 Å in one and 1.327 Å in the second molecule of the pair. These values are very unusual. There have been several earlier efforts to find a relation between the amount of positive
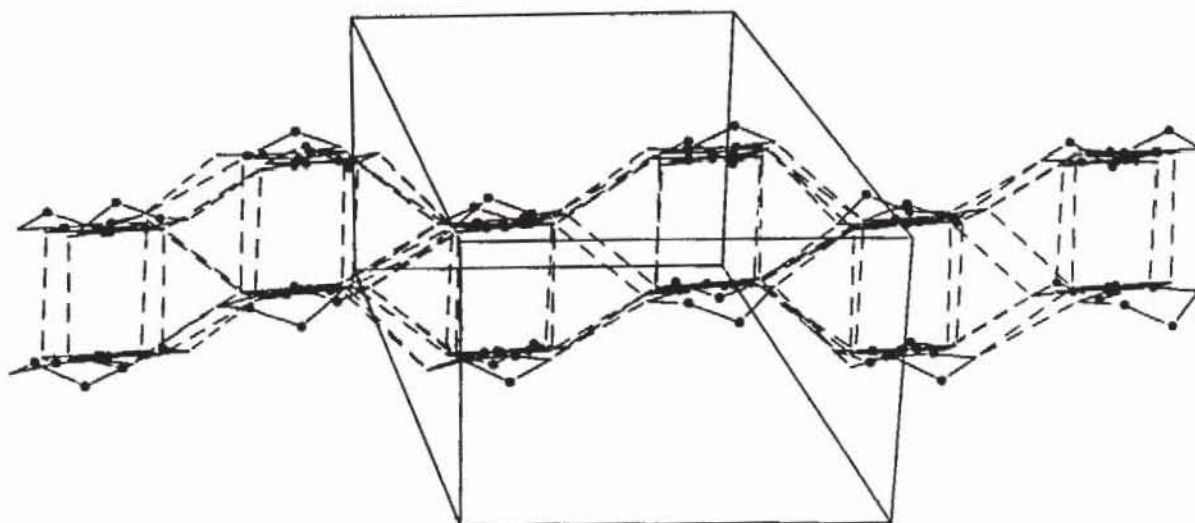
Fig. 4. S....S contacts < 3.8 Å between pairs of BEDT–TTF moieties.
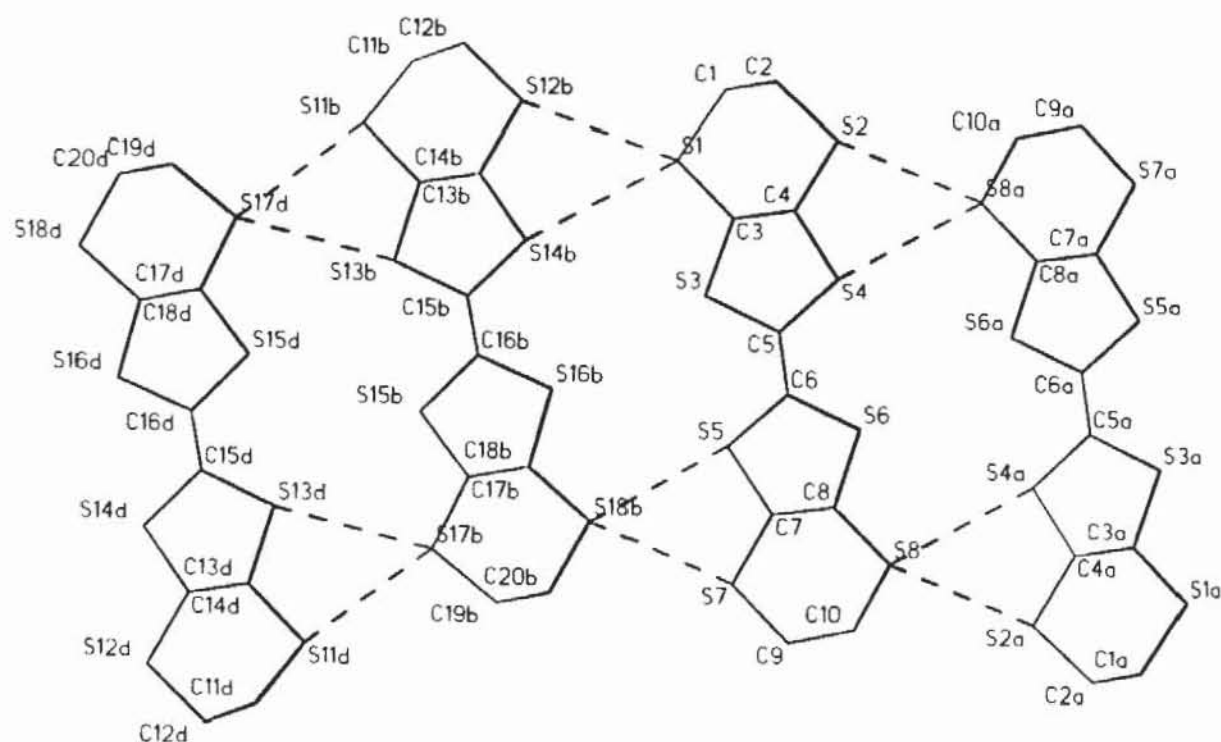
Fig. 5. The shortest S....S contacts between the columns (S_2–S_{8a} = 3.432 Å, S_5–S_{18b} = 3.382 Å and S_7–S_{18b} = 3.373 Å).

charge on the (BEDT–TTF)$^{n+}$ ions and the bond distances in these moieties [18, 19]. Compared to these earlier findings, the C=C distances reported here would suggest a negatively-polarized BEDT–TTF molecule. Since this is not reasonable for the DEDT–TTF moieties in the title compound, the determination of charge densities on the basis of bond distances in the BEDT–TTF salts has to be treated with caution. Either packing effects or the charge on the counterion (in our exceptional case *two*), which may lead to molecular distortions or polarizations, seem to play an important part in the bond distances too.
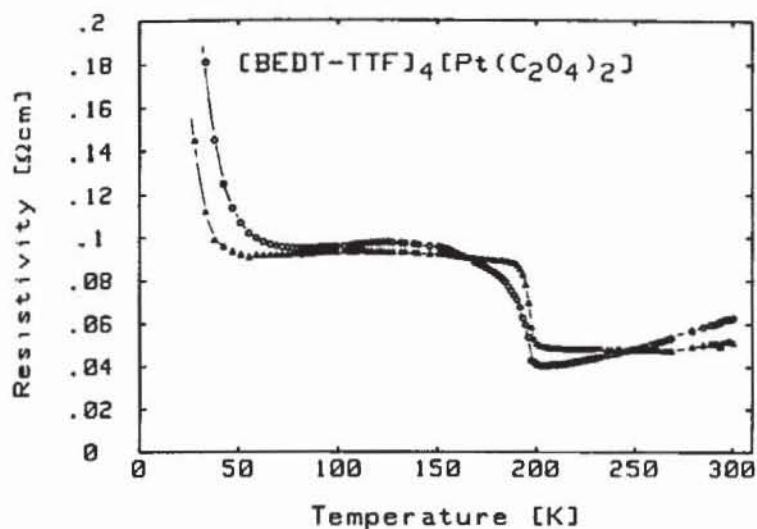
Fig. 6. Temperature dependence of the resistivity of two typical crystals of [BEDT-TTF]$_4$[Pt(C$_2$O$_4$)$_2$].

Figure 6 shows the temperature dependence of the resistivity of two typical crystals of our samples. The room-temperature conductivity σ_{300} is about 20 S/cm. For both crystals a weak decrease of the resistivity is observed by lowering the temperature down to 200 K. Such a behaviour is typical for a metal.

At around 200 K both crystals show a relatively sharp resistivity increase, indicating a structural phase transition at this temperature. As pointed out later, e.s.r. and thermopower investigations support this conclusion. Since the resistivity decrease continues below 120 K, as can clearly be seen in the blow-up in Fig. 7, it seems that the phase transition again leads into a metallic state. This conclusion is again supported by the results of the thermopower measurements (Fig. 8).

It is evident from Fig. 7 that the resistivity increases by lowering the temperature below 80 K in one crystal, and below 60 K in the other. Since this resistivity increase occurs in different crystals at different temperatures,
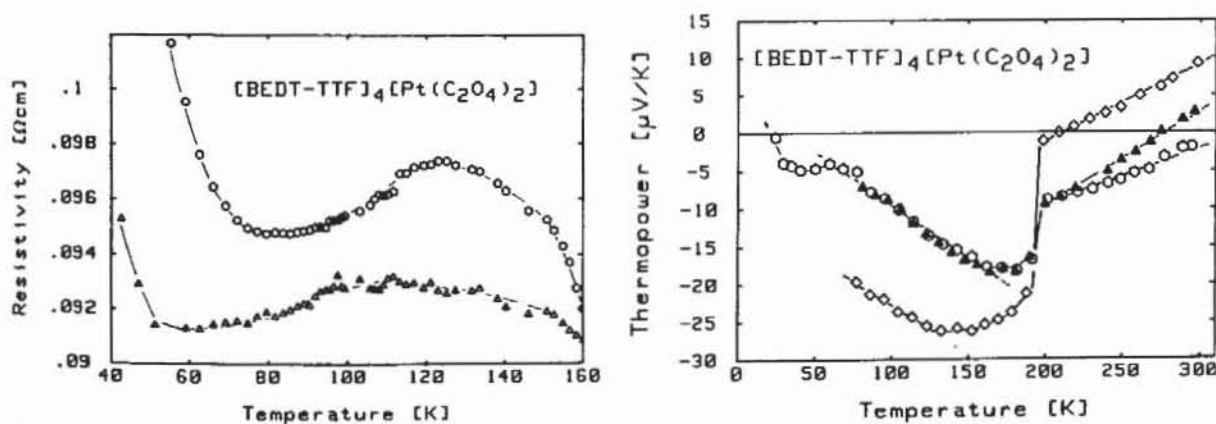
Fig. 7. Resistivity of the two crystals shown in Fig. 6 in the temperature range 40 - 160 K (expanded scale).

Fig. 8. Temperature dependence of the thermopower of three different crystals of [BEDT-TTF]$_4$[Pt(C$_2$O$_4$)$_2$].

it seems that a very broad phase transition into a semiconducting state exists (activation energy = 0.006 eV). The broadness of the transition might result from residual stresses due to the phase transition at 200 K, as well as from variations in crystal quality. A further indication for the existence of residual stresses in the crystals at lower temperatures is the fact that we were only in one case able to measure thermopower data below 70 K. With five other crystals only values down to 70 K could be obtained.

Figure 8 shows the temperature dependence of the thermopower of three crystals in the temperature range 20 - 300 K. Above 200 K the thermopower is directly proportional to the temperature, as expected for a metal. The sharp decrease at 200 K indicates the above-mentioned phase transition. In the lower temperature regime (70 - 140 K) the thermopower is again linearly proportional to the temperature as in a metal. Above 200 K the conductivity seems to be dominated by holes (positive thermopower at room temperature), while below 200 K the conductivity might be dominated by electrons. This change in charge carriers at the phase transition could be due to an opening of a gap in the conduction band, resulting in a different conduction band filling. In the crystal measured down to 20 K, the phase transition into the semiconducting state at about 60 K can be clearly seen.

The e.s.r. results are presented in Figs. 9 - 11. At room temperature the e.s.r. linewidth is weakly angle dependent and varies between 43 and 46 G. Figure 9 shows the temperature dependence of the e.s.r. linewidth starting with a room-temperature value of 43 G. By lowering the temperature the e.s.r. linewidth decreases to a value of about 3.5 G at 4.2 K. This is a typical behaviour expected for a quasi two-dimensional metal. Around 200 K a sharper decrease of the linewidth seems to occur, which in our opinion is due to the above-mentioned phase transition. The otherwise monotonic decrease of the linewidth with decreasing temperature can be attributed to temperature-dependent scattering processes. Therefore, the e.s.r. linewidth might be described by the Elliot formula for the spin relaxation in metals:
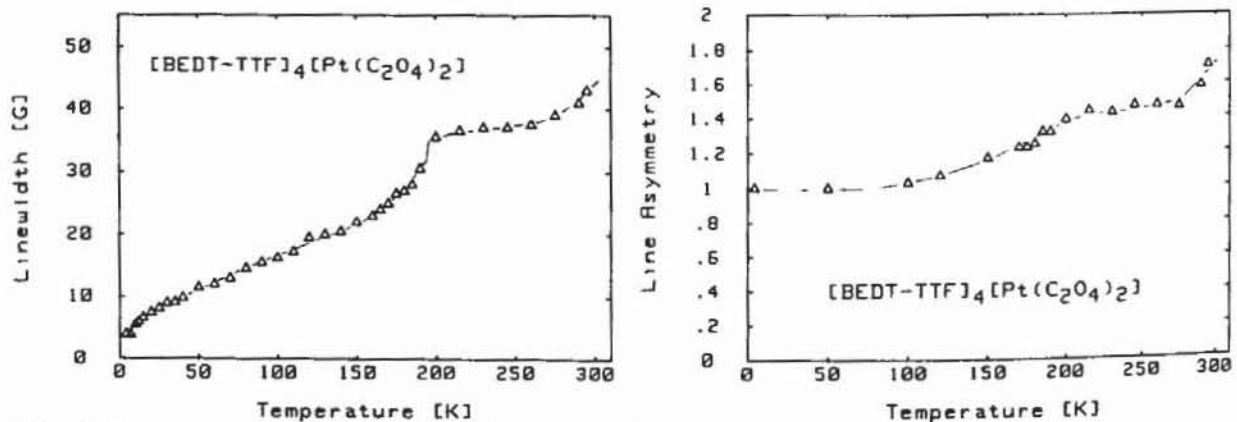
$$\Delta H = (\Delta g)^2 \tau^{-1}/\gamma$$

Fig. 9. Temperature dependence of the e.s.r. linewidth.

Fig. 10. Temperature dependence of the asymmetry of the e.s.r. line (Dyson-type e.s.r. line).

where $\Delta g = g - 2.0023$ measures the spin–orbit coupling, γ is the electron gyromagnetic ratio and τ^{-1} the scattering rate of the conduction electrons. At room temperature the e.s.r. line shows the typical Dyson-like asymmetry usually observed in metals. The temperature dependence of the asymmetry of the e.s.r. line is shown in Fig. 10. As can be seem from this diagram, the line becomes symmetric with a Lorentzian shape below 100 K in the region where the crystals become semiconducting.

Figure 11 shows the temperature dependence of the spin susceptibility as obtained from the e.s.r. measurements. Above and below 200 K the susceptibility is more or less temperature independent, while at 200 K a weak decrease appears. This result supports the assumption of a metal-to-metal phase transition at 200 K. The susceptibility is even constant below 60 K but at temperatures below 20 K an increase (probably due to paramagnetic impurities) is observed. These paramagnetic impurities might be responsible for the nearly temperature-independent behaviour of the susceptibility even in the semiconducting region.
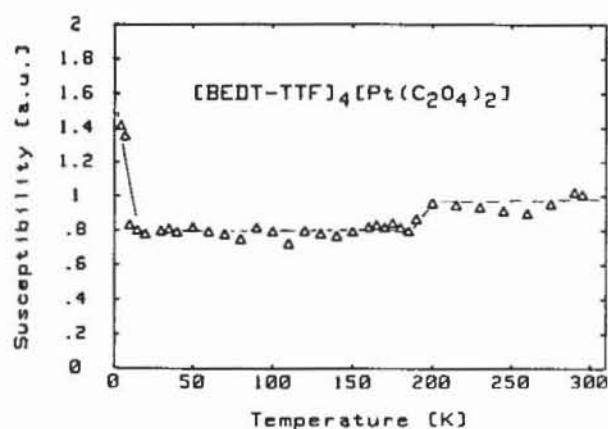

Fig. 11. Temperature dependence of the spin susceptibility (arbitrary units).

It should be mentioned that during the e.s.r. investigations we found a second crystallographic phase, which shows an e.s.r. linewidth of about 20 G at room temperature. Further investigations of this phase are in progress.

Conclusion

So far there have been only a very few attempts to react the doubly-charged anionic metal complexes, which are well known in the realm of one-dimensional 'inorganic' molecular metals, with organic donors [5, 20, 21]. Doubly-charged negative counterions seem to have a strong influence on the charge distribution in the 'organic part' of BEDT–TTF salts. Though the general features of the structure are as 'usual', the structural details are very different. To the best of our knowledge this is the first example of a metallic BEDT–TTF salt with a doubly negatively-charged counterion whose molecular structure has been unambiguously characterized. The solids with

'polymeric' anions [2, 3, 22, 23] with charges distributed over several metal centres are considered as a separate group, because the charge density on a special site in the counterion is difficult to determine.

There is one other example of this type of compound: $[BEDT-TTF]_4$-$[Pt(CN)_4]$ [5, 13]. One phase of this solid turned out to be a semiconductor. In one of the phases of the latter material, we again found two crystallographically different BEDT–TTF moieties with very different and comparatively short (1.306 and 1.350 Å) C=C central double bonds [13]. It is very surprising to note that despite the strongly alternating bonds in adjacent BEDT–TTF moieties and the clear pairing of these non-equivalent units along the stacks in the $[Pt(C_2O_4)_2]^{2-}$ derivative, a metallic behaviour results. On the basis of rules developed so far to predict high conductivity in molecular metals (regular, mixed valence stacks), one has to assume that the conduction path in the new compound follows solely along the intermolecular S–S contacts *perpendicular* to the stacks. The results obtained here and earlier [13] show that the molecular structure and physical behaviour of the BEDT–TTF salts with doubly-charged negative counterions are quite different from those of their mono-anionic 'relatives'. We will try to find out more about these special materials by using other planar platinum complexes as counterions.

Acknowledgements

References

1 S. S. P. Parkin, E. M. Engler, R. R. Schumaker, R. Lagier, V. Y. Lee, J. C. Scott and R. L. Greene, *Phys. Rev. Lett.*, 50 (1983) 270.

2 U. Geiser, H. H. Wang, K. M. Donega, B. A. Anderson, J. M. Williams and J. F. Kwak, *Inorg. Chem.*, 25 (1986) 401.

3 (a) L. I. Buravov, A. V. Zvarykina, M. V. Kartsovnik, N. D. Kushch, V. N. Laukhin, R. M. Lobkovskaya, V. A. Merzhanov, D. N. Fedutin, R. P. Shibaeva and E. B. Yagubskii, *Zh. Eksp. Teor. Fiz.*, 92 (1987) 594.
   (b) R. P. Shibaeva and R. M. Lobkovskaya, *Kristallografiya*, 33 (1988) 408.

4 M. Lequan, R. M. Lequan, G. Maceno and P. Delhaes, *Chem. Soc. Chem. Commun.*, (1988) 174.

5 R. P. Shibaeva, R. M. Lobkovskaya, V. E. Korotkov, N. D. Kushch, E. B. Yagubskii and M. K. Makova, *Synth. Met.*, 27 (1988) A457.

6 M. A. Beno, M. A. Firestone, P. C. W. Leung, L. M. Sowa, H. H. Wang, J. M. Williams and M.-H. Whangbo, *Solid State Commun.*, 57 (1986) 735.

7 *Proc. ICSM '88, Santa Fe, NM, U.S.A., June 26 - July 2, 1988*, Synth. Met., 27 - 29 (1988/89).

8 H. Urayama, H. Yamochi, G. Saito, K. Nozawa, T. Sugano, M. Kinoshita, S. Saito, K. Oshina, A. Kawamoto and J. Tanaka, *Chem. Lett.*, (1988) 55.

9 S. Gärtner, E. Gogu, I. Heinen, H. J. Keller, T. Klutz and D. Schweitzer, *Solid State Commun.*, 65 (1988) 1531.

10 J. M. Williams, A. J. Schultz, A. E. Underhill and K. Carneiro, in J. S. Miller (ed.), *Extended Linear Chain Compounds*, Vol. 1, Plenum Press, New York, 1982, p. 73.

11 A. E. Underhill, D. M. Watkins, J. M. Williams and K. Carneiro, in J. S. Miller (ed.), *Extended Linear Chain Compounds*, Vol. 1, Plenum Press, New York, 1982, p. 119.

12 A. E. Underhill, in P. Delhaes and M. Drillon (eds.), *Organic and Inorganic Low-Dimensional Crystalline Materials, NATO-ASI Series B*, Vol. 168, Plenum Press, New York, 1987, p. 17, and refs. therein.

13 S. Gärtner, I. Heinen, D. Schweitzer, H. J. Keller, R. Niebl and B. Nuber, *Z. Naturforsch.*, to be published.

14 G. M. Sheldrick, *SHELXTL. An Integrated System for Solving, Refining and Displaying Crystal Structures from Diffraction Data*, Univ. Göttingen, F.R.G., 1983.

15 *International Tables for X-Ray Crystallography*, Vol. IV, Kynoch Press, Birmingham, 1974. (Present distributor: D. Reidel, Dordrecht.)

16 (a) K. Bender, D. Schweitzer and H. J. Keller, *J. Phys. (Paris) Colloq.*, 44 (1983) C3 - 1433.
(b) K. Bender, *Diplomarbeit*, Universität Heidelberg, 1983.

17 A. Bondi, *J. Phys. Chem.*, 68 (1964) 441.

18 J. M. Williams, H. H. Wang, T. J. Emge, U. Geiser, M. A. Beno, P. C. W. Leung, K. D. Carlson, R. J. Thorn, A. J. Schultz and M.-H. Wangbo, *Prog. Inorg. Chem.*, 35 (1987) 51.

19 T. C. Umland, S. Allie, T. Kuhlmann and P. Coppens, *J. Phys. Chem.*, in press.

20 F. Wudl, *J. Am. Chem. Soc.*, 97 (1975) 1962.

21 K. Urayama, A. Tanaka, G. Matsubayashi and T. Tanaka, *Inorg. Chim. Acta*, 97 (1985) 201.

22 A. Weber, *Dissertation*, Universität Heidelberg, 1985.

23 U. Geiser, H. H. Wang, L. E. Gerdom, L. A. Firestone, K. S. Webb, J. M. Williams and M.-H. Whangbo, *J. Am. Chem. Soc.*, 107 (1985) 8305.